

AD715630

## THE EARLY DETECTION OF FATIGUE DAMAGE

## THIRD SEMIANNUAL REPORT

1 JUNE 1970 - 30 NOVEMBER 1970

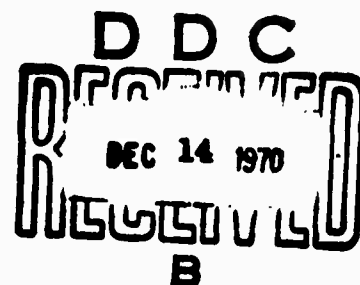
SPONSORED BY

ADVANCED RESEARCH PROJECTS AGENCY

ARPA ORDER NO. 1244

PROGRAM CODE NO. 8D10

Reproduced by  
NATIONAL TECHNICAL  
INFORMATION SERVICE  
Springfield, Va. 22151



Los Angeles Division  
North American Rockwell

THIS DOCUMENT IS UNCLASSIFIED  
DATE 10/10/01 BY 1045  
DISTRIBUTION IS UNRESTRICTED

**BEST  
AVAILABLE COPY**

This document may not be reproduced or published in any form, in whole, or in part without prior approval of the Government. Since this is a technical management report, this information herein is tentative and subject to changes, corrections, and modifications.

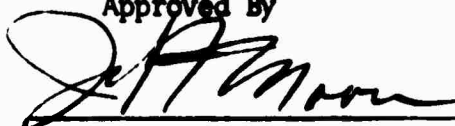
CLASSIFICATION		
GROUP	GROUP NUMBER	
DOC	DOC NUMBER	
UNCLASSIFIED	<input type="checkbox"/>	
JUSTIFICATION		
BY	per <i>Tekam</i>	
DISTRIBUTION/AVAILABILITY CODES		
DECL	AVAIL	and/or SPECIAL
1		

THE EARLY DETECTION OF FATIGUE DAMAGE

Third Semiannual Report

1 June 1970 - 30 November 1970

Approved By



John F. Moore  
Program Manager

DATE 30 November 1970  
NO. OF PAGES vi+38



Los Angeles Division  
North American Rockwell

International Airport, Los Angeles, California 90008, (213) 670-8151

## FOR:WORD

This is the third technical management report on a study for the development of methods for the early detection of fatigue damage, carried out by the Los Angeles Division of North American Rockwell Corporation. This research was supported by the Advanced Research Projects Agency of the Department of Defense under ARPA Order 1244, Program Code 8D10 and was monitored by the Air Force Materials Laboratory, LLN, under Contract F33615-68-C-1706. Lt. J. W. Bohlen was the Air Force Project Engineer. This report covers the period 1 June 1970 to 30 November 1970.

The program is being conducted by the Materials and Producibility Department, N. Klimmek, Manager, under the direction of Mr. J. F. Moore, Program Manager. The work described in this report was carried out by Mr. J. F. Moore, Dr. S. Tsang, Mr. F. M. Coate, Mr. D. S. Weinstein, and Mr. R. C. Sapp. Acknowledgment is also due to Dr. S. Hoenig, Professor of Electrical Engineering, University of Arizona, for his outstanding technical support.

## ABSTRACT

This report describes the continuing effort to develop nondestructive test methods capable of determining the extent of fatigue damage and providing a means of predicting the future safe life of aerospace materials and structures. During this report period, the fatigue process in 1100-O aluminum was studied by means of exoelectron emission and acoustic emission measurements. The exoelectron observations were by means of measuring the current produced by fatigue damage in air; the acoustic emission measurement was based on the number of acoustic events occurring in selected time intervals during fatigue. It appears that there is a trend indicative of a stress-independent relationship between the change of exoelectron emission current and the percentage of the spent fatigue life based on the current after a selected number of cycles. The intensity of acoustic emission was shown to increase or decrease by orders of magnitude during the fatigue life. The first significant change of acoustic emission was apparently correlatable to 8 to 20 percent of the specimen fatigue life. The continuing metallographic examination confirmed that surface slip striations appear very early in the fatigue process and appear to directly correlate with the exoelectron emission phenomenon.

## TABLE OF CONTENTS

Section		Page
I	INTRODUCTION	1
II	EXPERIMENTAL EQUIPMENT	2
	Fatigue Test Unit	2
	Exoelectron Emission	2
	Acoustic Emission	4
III	SPECIMEN MATERIAL AND PREPARATION	10
	Materials	10
	Specimens	10
IV	EXPERIMENTAL RESULTS AND DISCUSSION	12
	Exoelectron Emission	12
	Acoustic Emission	21
	Ultrasonic Methods	27
	Metallographic Examination	31
	Fatigue Tests	32
V	SUMMARY AND CONCLUSIONS	36
VI	FUTURE WORK	38

## LIST OF ILLUSTRATIONS

Figure	Title	Page
1	Schematic Diagram of Electrodeless Emission Measurement System....	3
2	Electrodeless Emission Measurement System.....	5
3	Specimen in Electrodeless Emission and Acoustic Emission Test.....	6
4	Block Diagram of Acoustic Emission Measurement System.....	8
5	Acoustic Emission Measurement System.....	9
6	Electrodeless Emission of 1100-O Aluminum in Fatigue Test at 11,000 Pounds per Square Inch.....	14
7	Electrodeless Emission of 1100-O Aluminum in Fatigue Test at 10,540 Pounds per Square Inch.....	15
8	Electrodeless Emission of 1100-O Aluminum in Fatigue Test at 11,400 Pounds per Square Inch.....	17
9	Relation of Percentage Change of Current to Percentage Change of Fatigue Life for 1100-O Aluminum.....	19
10	Acoustic Emission of 1100-O Aluminum in Fatigue Test at 11,400 Pounds per Square Inch.....	22
11	Acoustic Emission of 1100-O Aluminum in Fatigue Test at 11,000 Pounds per Square Inch.....	23
12	Acoustic Emission of 1100-O Aluminum in Fatigue Test at 10,540 Pounds per Square Inch.....	24
13	Optical Micrographs of Fatigued 1100-O Aluminum Specimens (250X).....	33
14	Electron Micrographs of Fatigued 1100-O Aluminum Specimens (6,400X).....	34



## LIST OF TABLES

Table	Title	Page
I	Summary of Fatigue Test Results for 1100-O Aluminum.....	13
II	Summary of Acoustic Emission Measurement for 1100-O Aluminum in Fatigue Test.....	26

## Section I

## INTRODUCTION

The phenomena of fatigue of metals and alloys have been an important consideration in the application of aerospace materials. The possibility of the early detection of fatigue damage could significantly improve the material utilization and system reliability. Most available methods are related to the detection of actual cracks which, however, generally appear late in the fatigue process.

The objective of this program is the development of methods suitable for the early detection of fatigue damage. During the first year of this program, the process of exoelectron emission during the fatigue deformation of aluminum under vacuum conditions and the propagation characteristics of ultrasonic surface waves were investigated to determine their potential for detecting fatigue damage. The process of exoelectron emission was shown to be most promising and was further studied, not in vacuum but in air, in order to adapt this process more conveniently for practical application as a non-destructive test technique. The acoustic emission of metals by fatigue stressing was also measured to determine its feasibility for detecting fatigue damage.

## Section II

## EXPERIMENTAL EQUIPMENT

FATIGUE TEST UNIT

The fatigue test unit was described in the final report for the first-year effort published as Technical Report AFML-TR-70-124. The specimen and instrumentation transducer for measuring the exoelectron emission in air were enclosed in the glass chamber (previously used for the fatigue tests in vacuum) in order to lessen air movement around the specimen to preclude drift of the emission current. The acoustic background noise level was also greatly reduced for the acoustic emission measurements.

EXOELECTRON EMISSION

The current of exoelectron emission of deformed metals is generally very small. It is necessary to stimulate the emission to enhance the current level so that it can be measured in air. A special current measuring system was devised (based on designs for a similar instrument developed by Professor S. Ikenig of the University of Arizona) to measure currents as small as  $10^{-14}$  ampere. The NR/LAD system (figure 1) uses an operational amplifier having field-effect transistors in the input stage. Current feedback through a very high precision resistor is used to null the input of the amplifier. The amplitude of the average voltage applied to the feedback resistor is a direct indicator of the current entering the collector plate from the specimen. The voltage is then converted to digital readings, using Electro Instruments

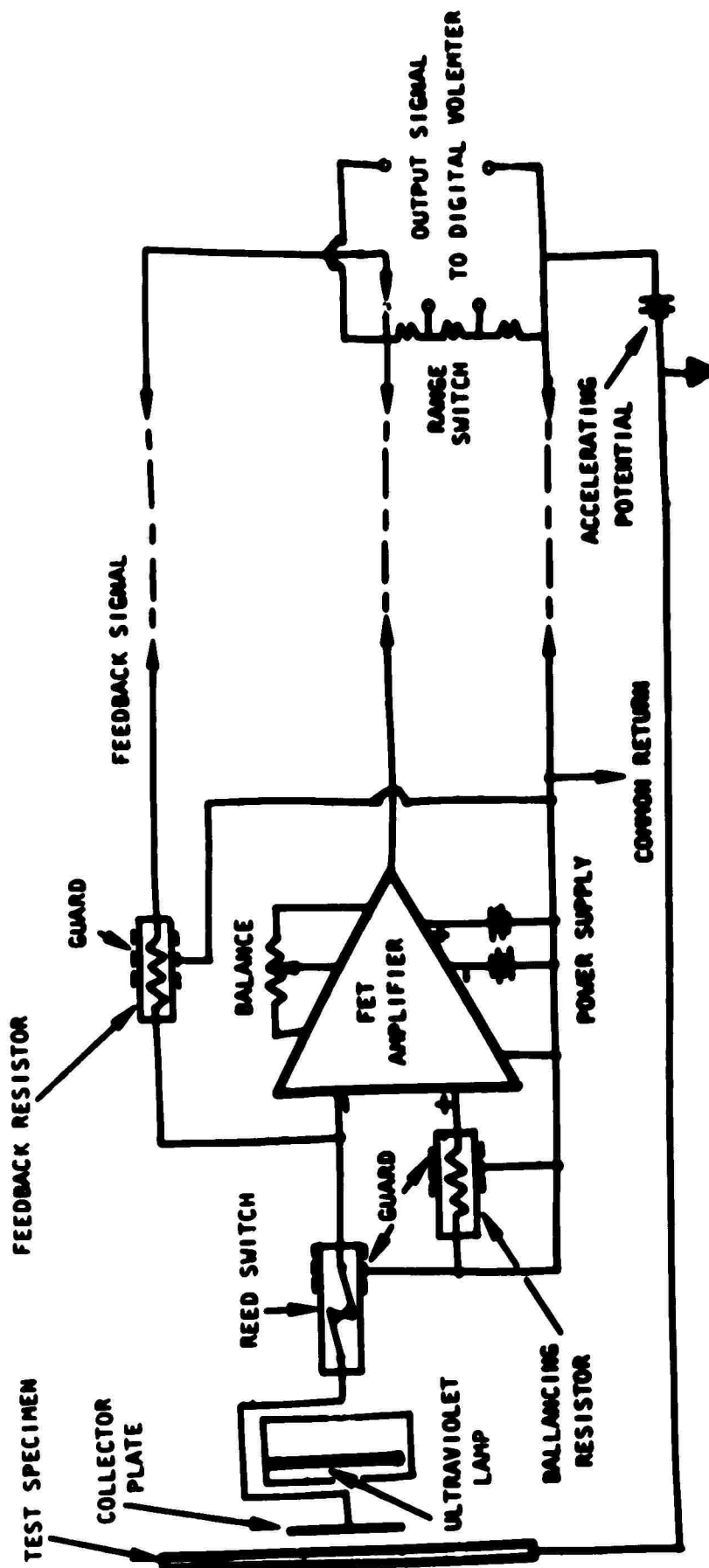


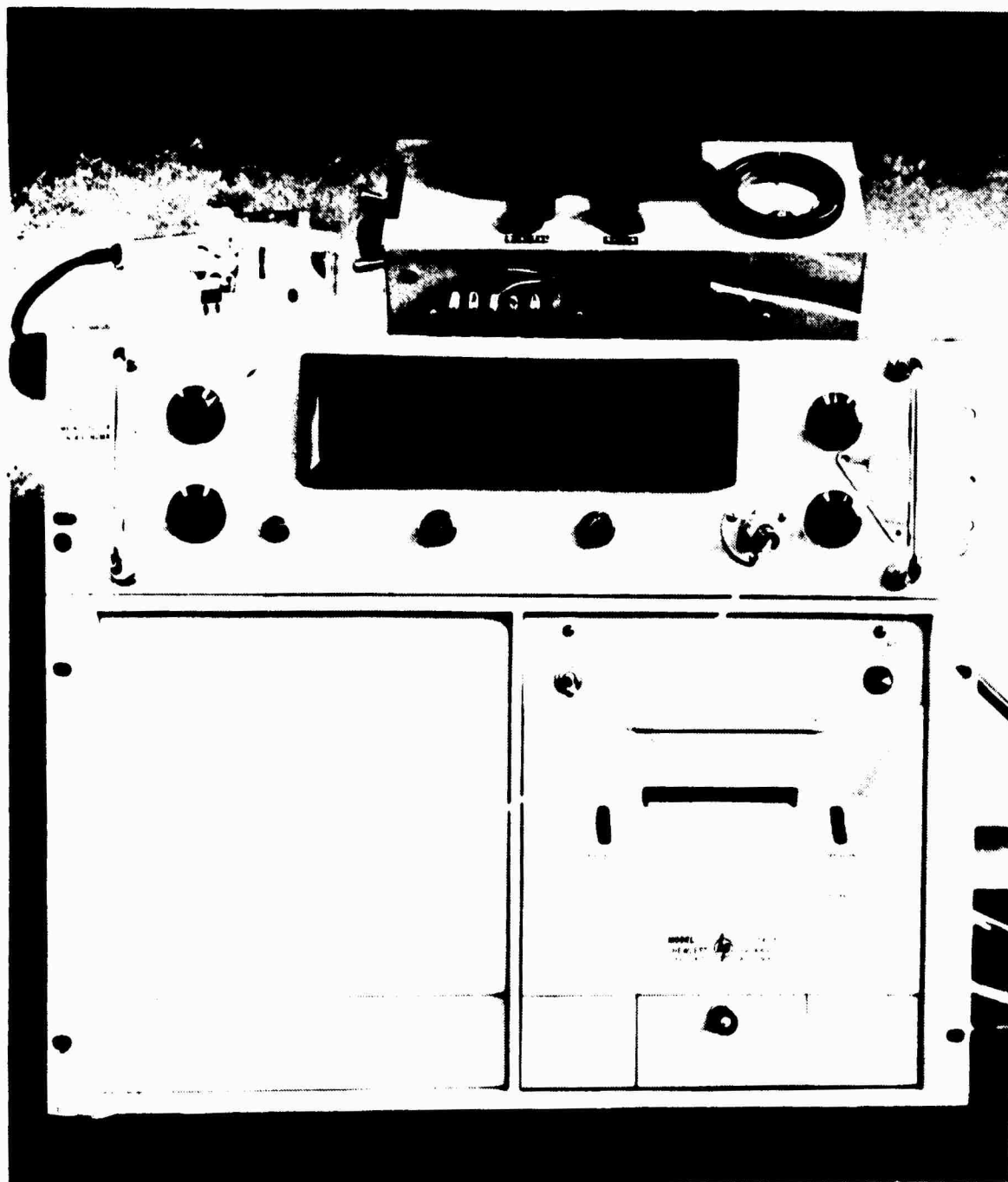
Figure 1. Schematic Diagram of Electrostatic Emission Measurement System

Model 8409 electronic digital voltmeter, and is printed on tape with Hewlett-Packard digital recorder Model 561A. The time interval between printing is controlled by the cycling of the hydraulic system of the fatigue test unit. A current reading is printed every  $10^1$ ,  $10^2$ ,  $10^3$ , or  $10^4$  fatigue cycles. Measurements of exoelectron emission during a test required three current ranges of  $10^{-12}$ ,  $10^{-11}$ , and  $10^{-10}$  ampere per volt of output. The ranges were manually selected. A photograph showing this measuring system enclosed in two boxes on top of the digital voltmeter and the recorder is reproduced in figure 2.

The exoelectron emission was stimulated with a short-wave ultraviolet pencil lamp source shielded in a metal box. The current collector plate consisted of a fine stainless steel screen having about 80 percent of open area. The ultraviolet light leaves the box through a 1/2-inch-diameter hole, passes through the screen, and impinges upon the middle portion of the test specimen. The distance between the specimen and the screen is maintained at one-fourth inch; the ultraviolet lamp is five-eighths inch further away from the screen. Figure 3 shows the specimen installed in the loading frame with the collector plate and the box housing the ultraviolet lamp.

#### ACOUSTIC EMISSION

The acoustic emission from the specimen during fatigue test was detected using a Dunigan acoustic emission transducer No. D-1408. This transducer is electrically shielded and has a differential output, so it is less susceptible



NOT REPRODUCIBLE

Figure 2. Exoelectron Emission Measurement System

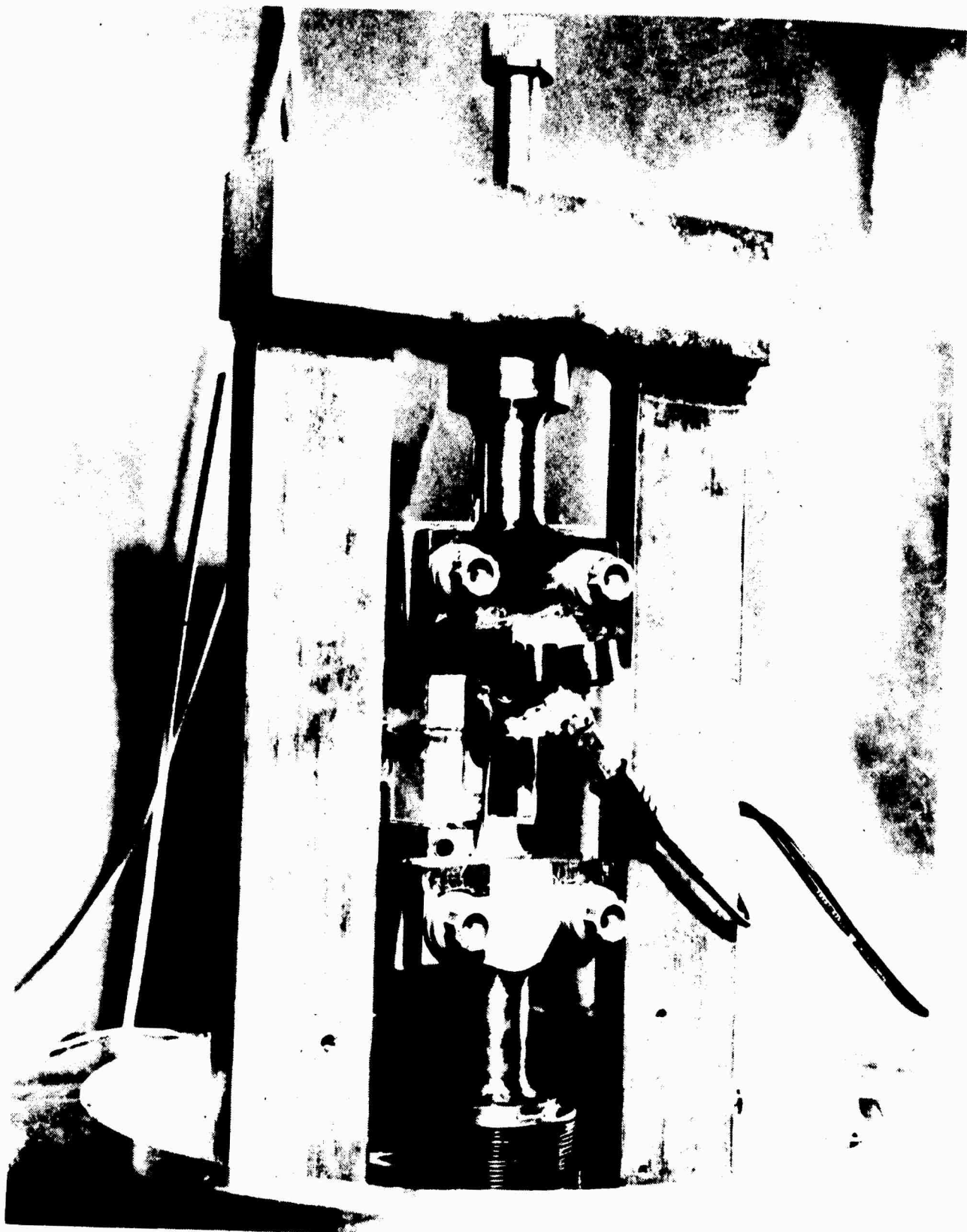


Figure 3. Specimen in Exoelectron Emission and Acoustic Emission Test

NOT REPRODUCIBLE

to electrical noise. In addition, it has a narrow bandwidth with a resonance frequency at approximately 210 kHz. The transducer is held in position on the specimen by a spring clip as shown in figure 3 and is acoustically coupled to the specimen surface with Apiezon-N grease.

The acoustic signal from the transducer is amplified by an oscilloscope preamplifier, fed into a counter, and recorded as the number of acoustic pulses. The time interval between printing (which is either  $10^1$ ,  $10^2$ ,  $10^3$ , or  $10^4$  fatigue cycles) is controlled in a similar manner as the printing of the digital voltmeter readings for exoelectron emission measurements. The printed number of counts indicates the total number of events that have taken place within the selected time interval. In the case of exoelectron emission, however, the recorded digital voltmeter reading is a measure of the current at the time of printing.

If needed, the total events of acoustic emission can be further broken down into a number of events occurring in any one cycle by converting the ac signal to dc and feeding the converted signal to a Visicorder. Each deflection on the recording graph indicates a number of pulses that are detected by the transducer at the time of recording. The height of the deflection is a measure of the acoustic emission power which has been generated. Figure 4 is a block diagram for measuring the acoustic emission, while figure 5 is a photograph showing the control box for controlling the time interval between printing, the oscilloscope, the counter, and the printer.



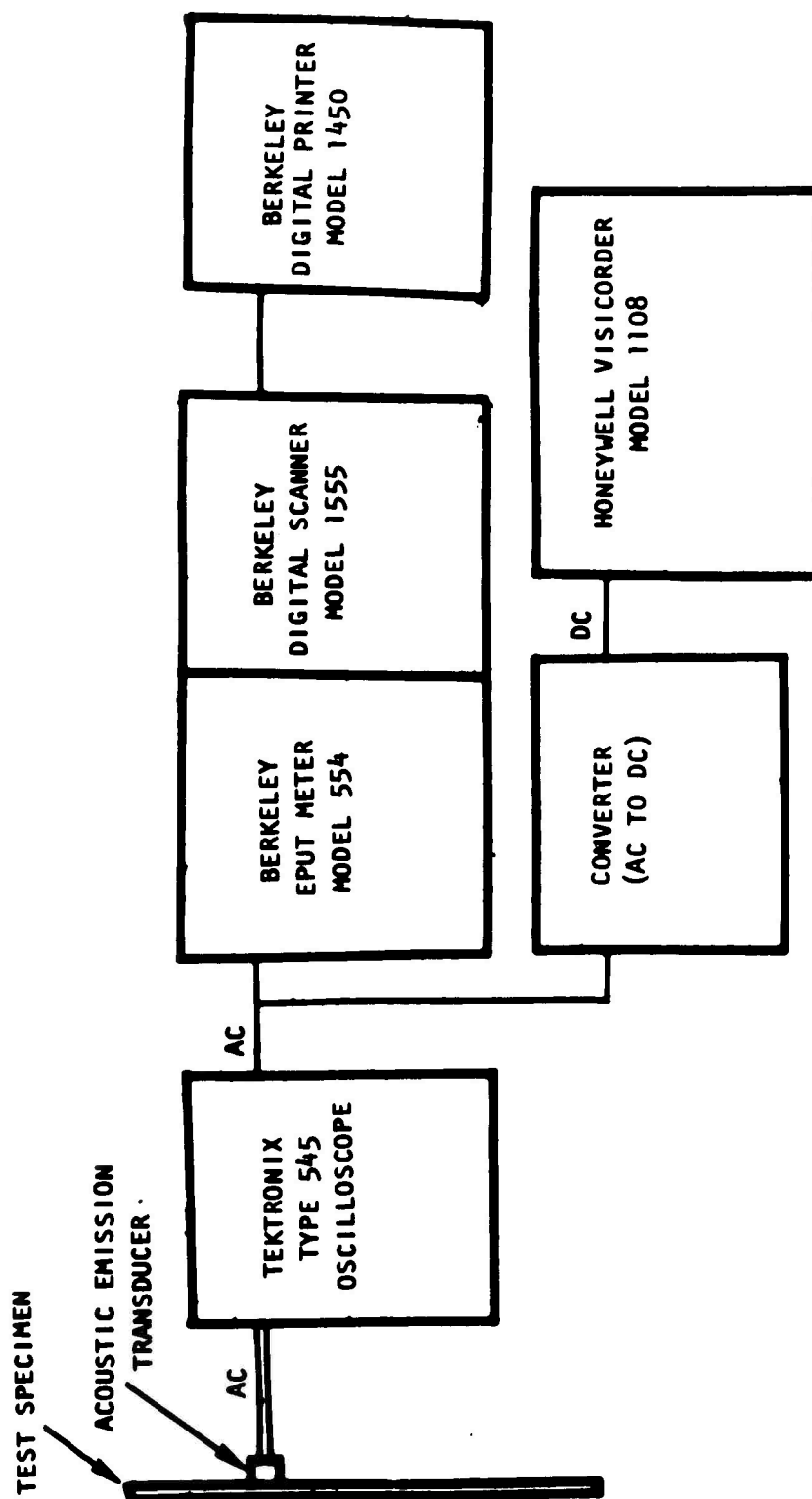


Figure 4. Block Diagram of Acoustic Emission Measurement System

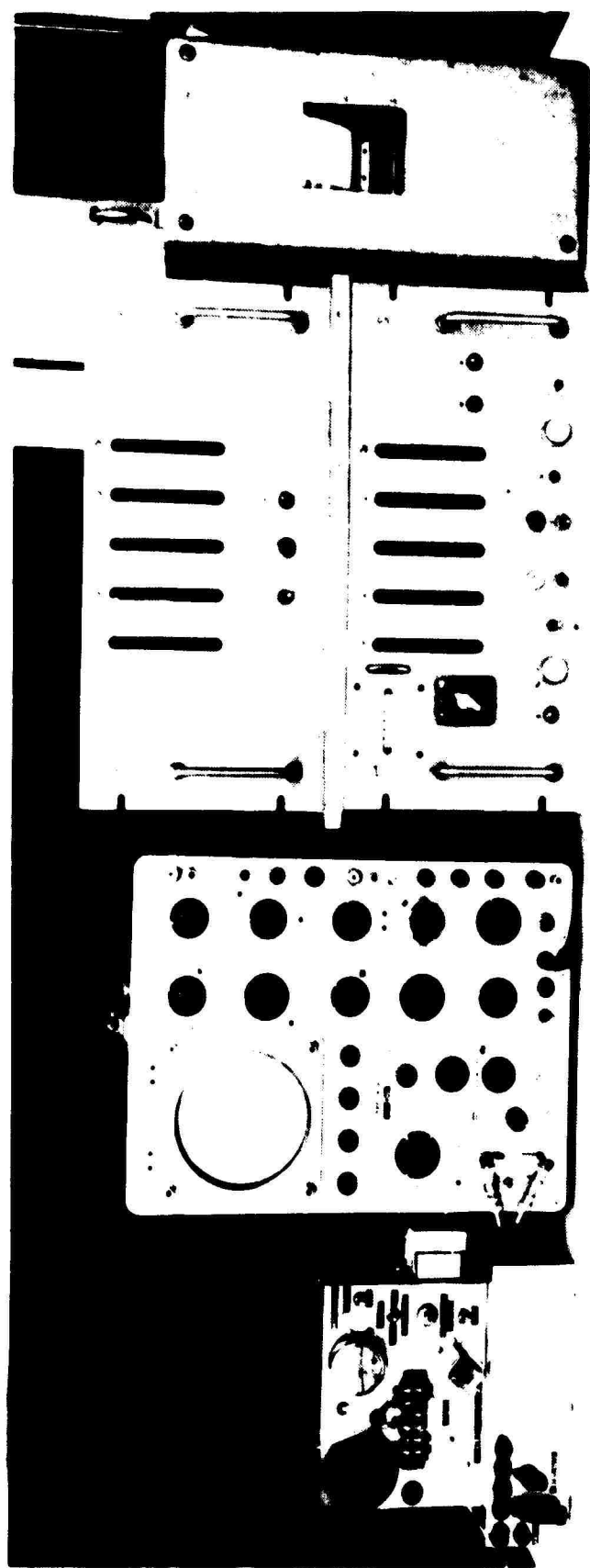


Figure 5. Acoustic Emission Measurement System

NOT REPRODUCIBLE

## Section III

## SPECIMEN MATERIALS AND PREPARATION

MATERIALS

Four materials, furnished by Aerojet-General Corporation, were used in the experimental work and included 1100-O aluminum, 7065-T6 aluminum alloy, mill annealed D6AC steel, and EI grade 6Al-4V titanium alloy in annealed condition. Their tensile properties are as follows:

Material	Yield Strength (psi)	Ultimate Strength (psi)
1100-O aluminum	—	13,000
7075-T6 aluminum alloy	70,000	80,000
D6AC steel	70,000	100,000
6Al-4V titanium alloy	130,000	140,000

SPECIMENS

The specimens fabricated by Aerojet-General Corporation used a straight 2-inch test section with a 1/2-inch width. A fillet of 1-inch radius joined the test section to the specimen end which is 1 inch wide. The nominal thickness of the aluminum and its alloy specimens was 0.09 inch, whereas that of the steel and titanium alloy specimens was 0.10 inch. This specimen configuration was found unsatisfactory since fatigue fracture repeatedly occurred at either the end of the test section or the fillet. Each side of test section was then notched with a 6-inch-radius cutter so that the smallest specimen

width between the notch roots was about 0.41 inch. The fillet radius was increased to 3 inches. Fatigue fracture of the modified specimen then took place at the middle reduced section.

The 1100-O aluminum specimens were either chem-milled or electropolished before test. Composition of the chem-milling solution on a 1-gallon basis is 20 ounces sodium hydroxide, 2 percent by weight sodium gluconate, and 2 percent by weight sodium sulfide. The temperature of the solution did not exceed 170° F. Electropolishing was carried out at a current density of 0.15 ampere per square centimeter in a bath containing 60 percent phosphoric acid and 40 percent sulfuric acid heated between 160° and 170° F.

The 7075-T6 aluminum alloy specimens were chem-milled in the same solution used for preparing the 1100-O aluminum specimens prior to test.

## Section IV

## EXPERIMENTAL RESULTS AND DISCUSSION

EXOELECTRON EMISSION

Eight 1100-O aluminum specimens were tested by fatiguing at varying stress levels. The exoelectron emission of each specimen was continuously measured in air during test. Table I summarizes the fatigue test results.

Prior to test, the background level for the exoelectron emission was established after the specimen was irradiated with short-wave ultraviolet light for at least 18 hours and the collector plate of the current measuring system was charged to positive 45-volt potential. This procedure was followed to insure that spurious electron emission due to specimen preparation or mounting was quiescent. Figure 6 shows the exoelectron emission curves for four 1100-O aluminum specimens subject to fatigue stressing at 11,000 psi. The emission current rises rapidly soon after start of the test, reaching the peak between 40 and 100 cycles. Thereafter, the emission intensity decreases gradually as cycling proceeds. After the current reaches the initial background level, it continues to drop until fatigue cracks form. The current first rises slowly and then rapidly as the cracks propagate through the test section, leading to complete specimen failure.

At the lower stress level of 10,540 psi, the exoelectron emission curves of 1100-O aluminum in fatigue deformation (figure 7) exhibit characteristics similar to the 11,000 psi data. At a higher stress level of 11,400 psi, the

Table 1

## SUMMARY OF FATIGUE TEST RESULTS FOR 1100-O ALUMINUM

Specimen	Surface Preparation	Maximum Stress (psi)	Number of Cycles at Failure
71	Electropolish	11,400	53,370
78	Electropolish	11,400	11,990
74	Chem-mill	11,000	345,430
80	Electropolish	11,000	696,500
82	Chem-mill	11,000	802,000
88	Chem-mill	11,000	271,000
85	Electropolish	10,540	761,100
86	Electropolish	10,540	336,490

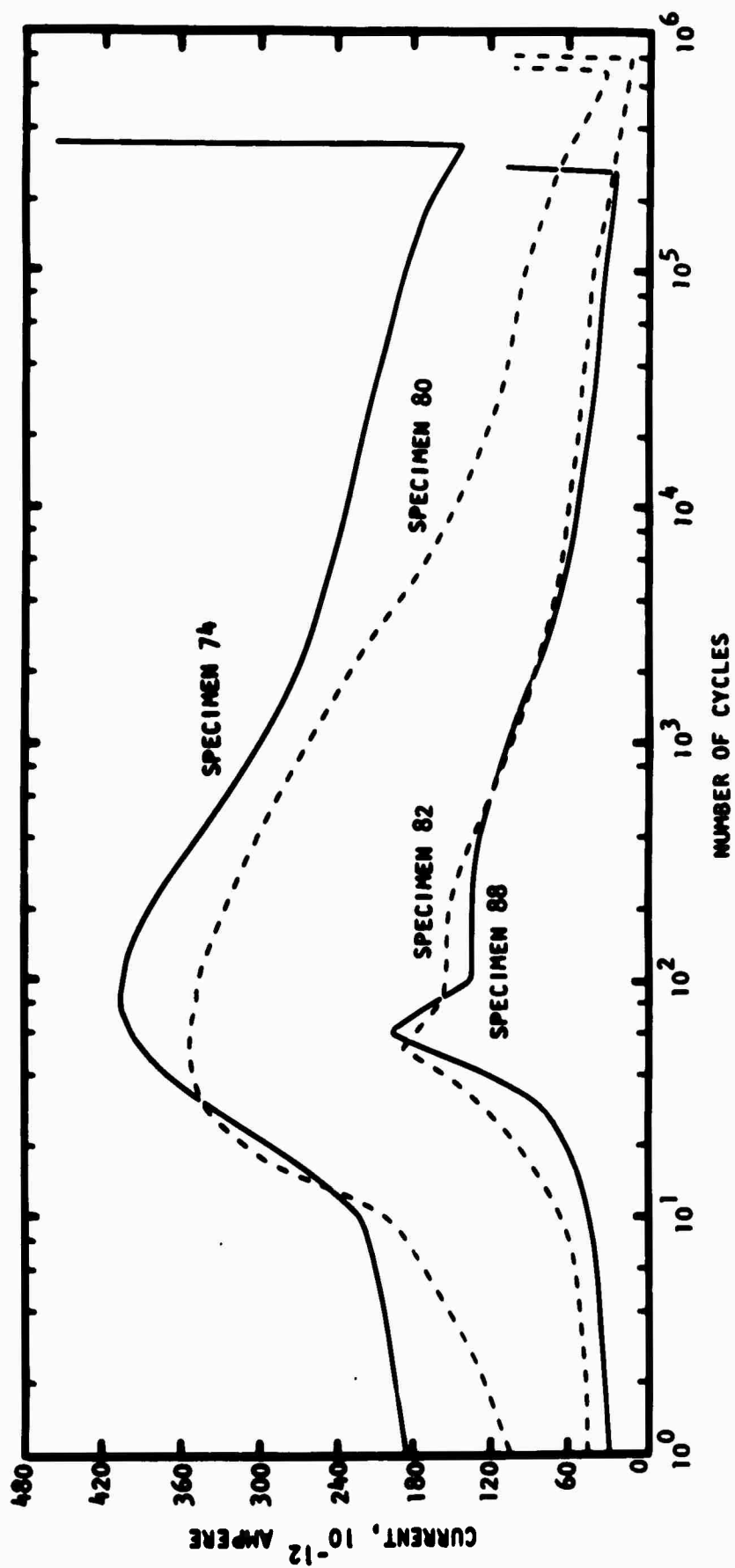


Figure 6. Exoelectron Emission of 1100-0 Aluminum in Fatigue Test at 11,000 lb/in.<sup>2</sup>

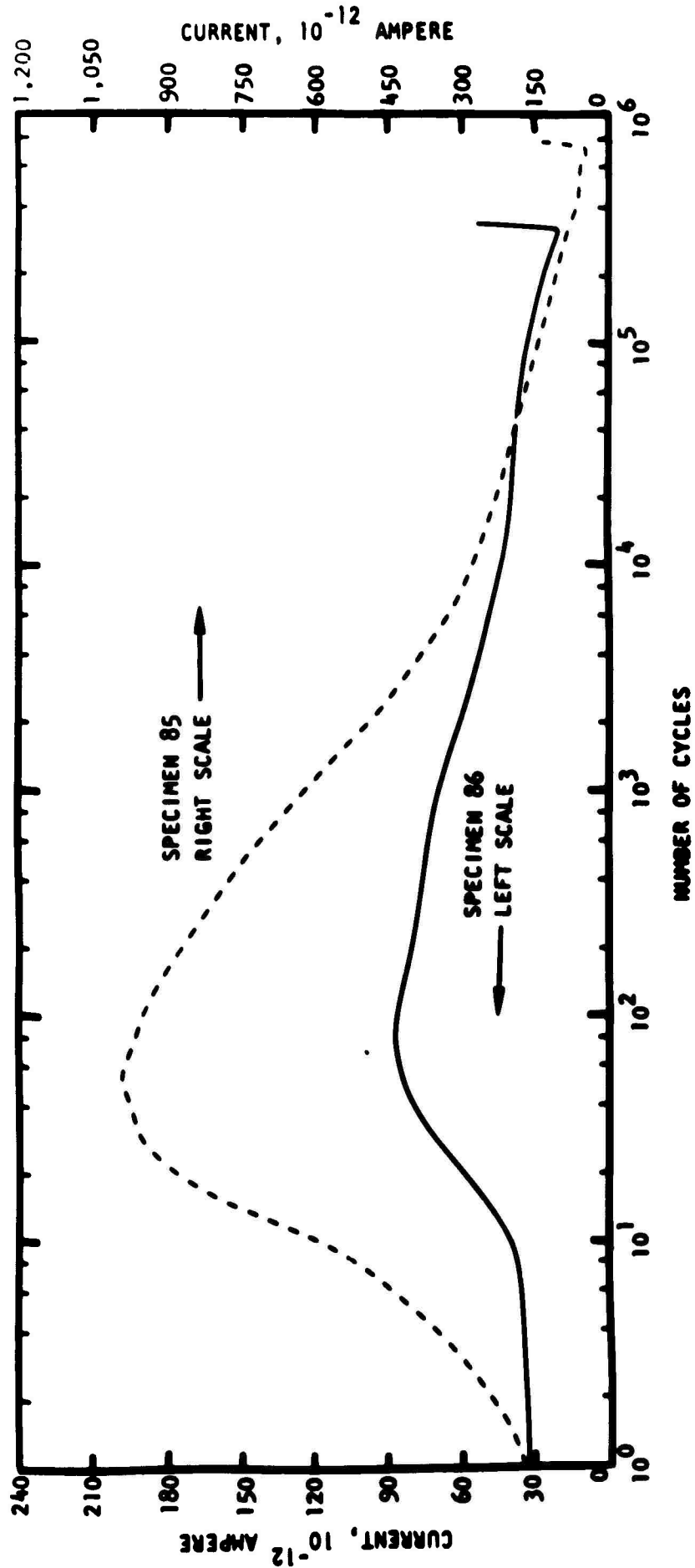


Figure 7. Exoelectron Emission of 1100-0 Aluminum in Fatigue Test at 10,540 lb/in.<sup>2</sup>



overall shape of the emission curve (figure 8) is repeated, but the emission current does not drop to the initial background level before it rises again due to the formation and propagation of fatigue cracks.

Table I and figures 6, 7, and 8 show that the exoelectron emission behavior of 1100-O aluminum by fatigue deformation in air is not influenced by the applied stress. Magnitudes of the emission current can vary appreciably for the specimens subject to equal stressing and same surface preparation. Regardless of the stress level, the current rises rapidly only in the first few hundred cycles. Since little fatigue damage is expected in such very short time, the rising portion of the emission curve was not included in the current analysis. An examination of figure 6 reveals that, after the elapse of the first 1,000 cycles, the emission curves tend to have similar decreasing trend. Therefore, the change of emission current was computed with reference to the current at 1,000 cycles rather than the background level prior to test.

At the stress level of 11,000 psi, the fatigue life of the specimens varies (table I), but, on the conservative side, a lower limit of life can be obtained from the two shorter lives for specimens 74 and 88. The average value of approximately  $3 \times 10^5$  cycles was, therefore, considered to be the typical fatigue life at 11,000 psi. The actual life used in analysis is  $2.99 \times 10^5$  cycles so that, by the subtraction of 1,000 cycles, the reference current is now the value at these cycles. The emission current at various number of cycles corresponding to certain percentages of life for the four specimens was noted on the record tape and the percent of current change

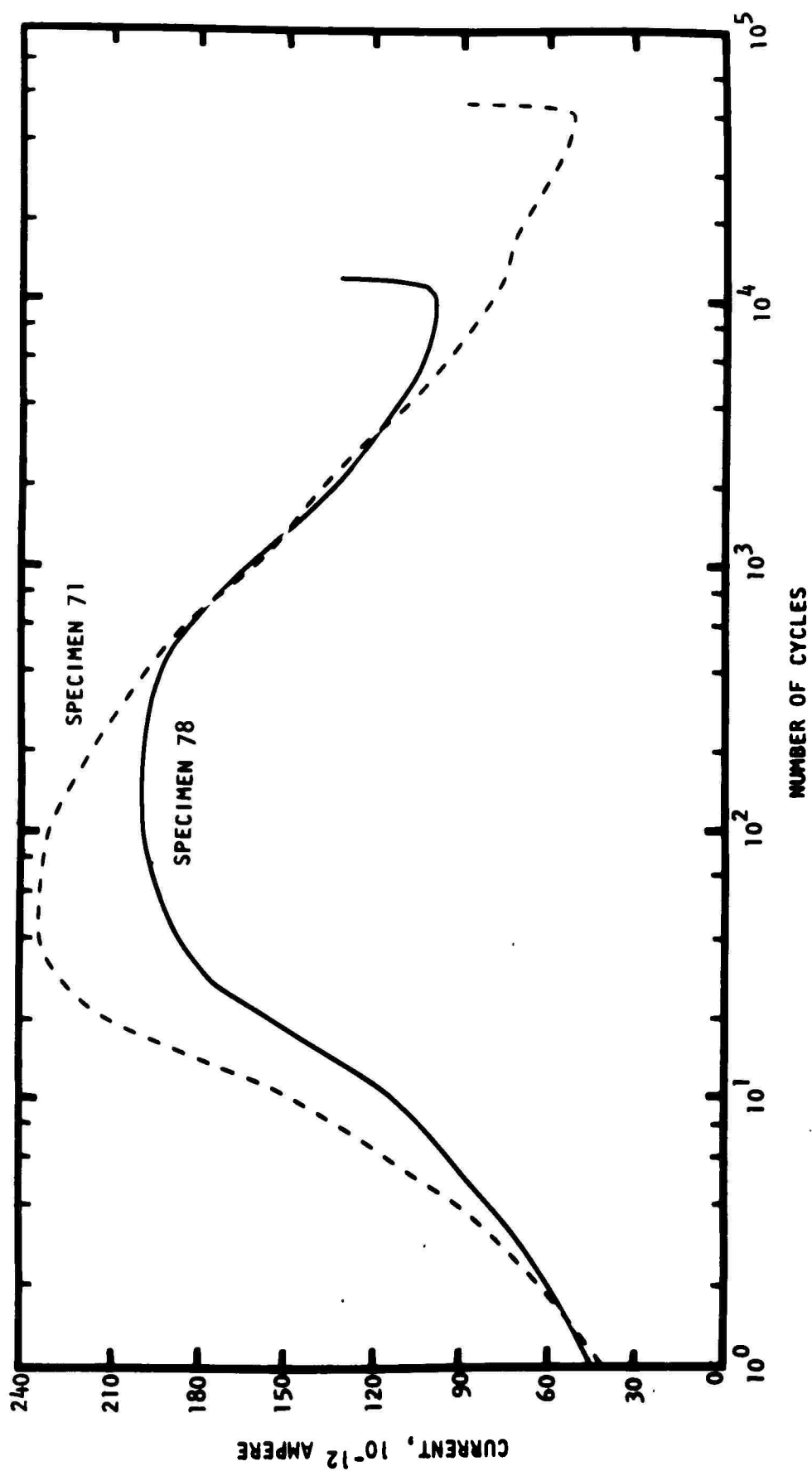


Figure 8. Exoelectron Emission of 1100-0 Aluminum in Fatigue Test at 11,400 lb/in.<sup>2</sup>

relative to the value at 1,000 cycles were computed and plotted versus the percentage of fatigue life in figure 9. Data points for specimens 80, 82, and 88 gather in a group; however, the data for specimen 74 does not fit and the reason for this discrepancy was not apparent.

A conservative estimated average fatigue life at the stress level of 10,540 psi (table I) is set at  $4 \times 10^5$  cycles. Again, the subtraction of 1,000 cycles results to a life  $3.99 \times 10^5$  cycles for the analysis. Changes of the emission current for specimen 86 are computed and also plotted in figure 9. The data points again fall in the group formed by those for specimens 80, 82, and 88. The emission data for specimen 85 are not analyzed since magnitudes of the current are excessively large in comparison with those for all remaining specimens tested at different stress levels (figure 7). It is not certain why specimen 85 had a very strong emission by fatigue deformation at relatively low stress level.

At 11,400 psi, the fatigue life for specimen 78 is about one-fourth the life for specimen 71. The rather short life may be ascribed to overstressing due to malfunctioning of the load valves in the hydraulic system, which failed at the end of this test. The fatigue life at 11,400 psi was set at  $5 \times 10^4$  cycles close to the life for specimen 71. The reference of emission current is shifted to 500 cycles since both specimens 71 and 78 emitted about the same amount current at 500 cycles. The life for analysis is consequently  $4.95 \times 10^4$  cycles. The change of current with fatigue life for specimen 71 is also included in figure 9.

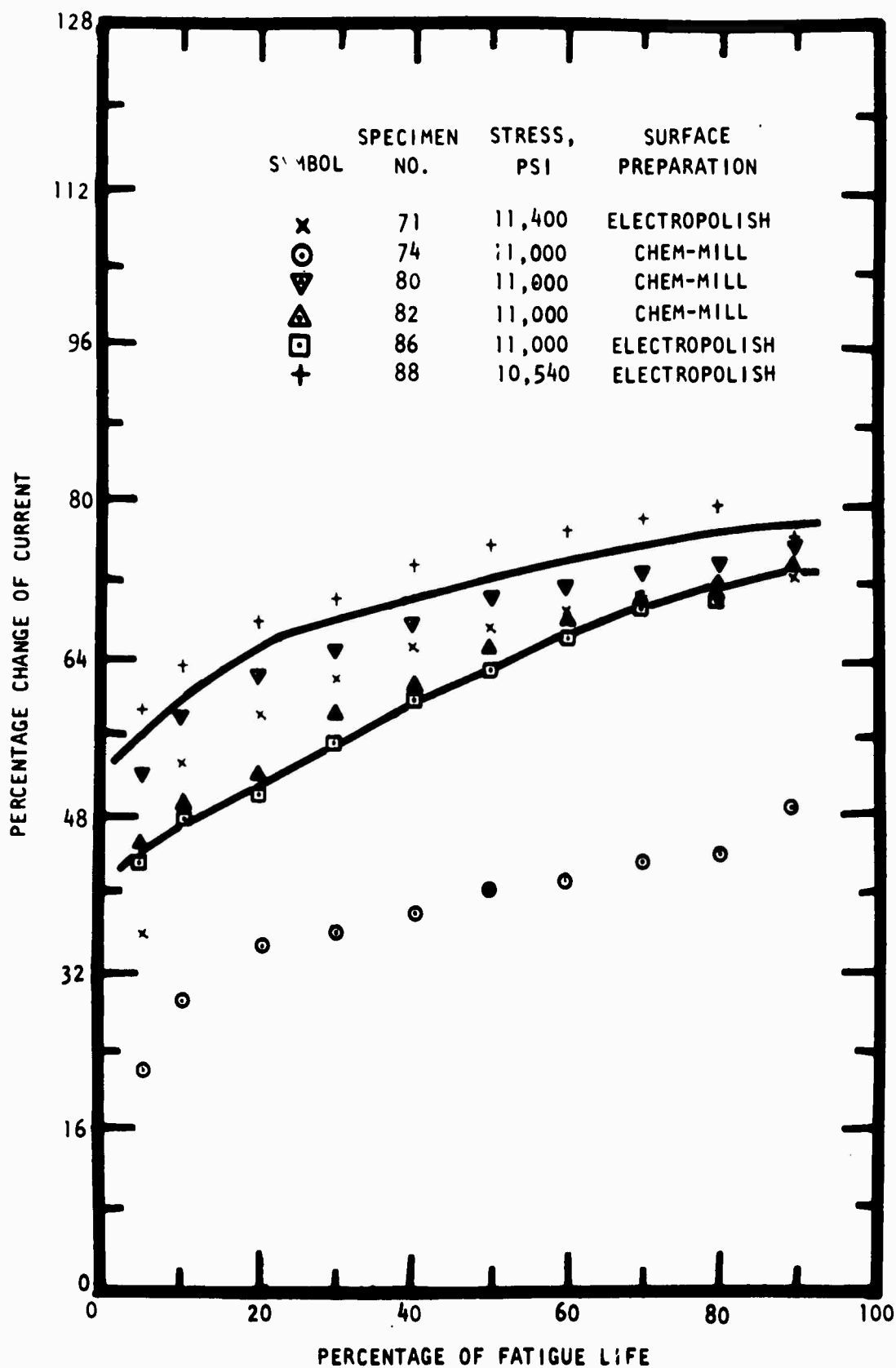


Figure 9. Relation of Percentage Change of Exoelectron Emission Current to Percentage of Fatigue Life for 1100-0 Aluminum

Figure 9 shows that it is possible to predict the remaining safe fatigue life of 1100-O aluminum by estimating the change of exoelectron emission current at the end of the spent life, if the change is based upon the current at the first few hundreds or thousands of cycles when the current decreases steadily after its initial rapid rise and fall.

It is believed that the relation of the emission current change to the percentage of fatigue life should be independent of applied stress levels. A number of specimens subject to fatigue deformation at differing stress levels exhibit the same percentage change of current after the elapse of various numbers of cycles. A single curve should tell what the percentages of life have been spent at these cycles. The remaining safe life can, therefore, be easily estimated. A trend approaching this idealized relation is clearly shown in figure 9, even though a band instead of a single curve is drawn to cover most of the data points. Therefore, the measurement of exoelectron emission in air during fatigue stressing is a promising tool for detecting early fatigue damage and assessing the remaining safe life at least for 1100-O aluminum.

There appears to be a similarity in the exoelectron emission curves for 1100-O aluminum by fatigue deformation in air and in vacuum. Both curves exhibit an early rapid rise and decay of the emission intensity, and again a rapid rise shortly before the specimen failure. Though a relationship between the change of emission intensity and the percentage of fatigue life for the tests in vacuum is not apparent, a few checks with the emission curves at stress levels above 10,540 psi indicate a possible existence of such stress-independent trend.

## ACOUSTIC EMISSION

The acoustic emission measurements on 1100-O aluminum specimens were conducted concurrently with exoelectron emission tests. The acoustic emission transducer was coupled to one face of the test section of the specimen, whereas the other face was illuminated with ultraviolet light to stimulate exoelectron emission. Before the test, the sensitivity of the counter (EPUT meter) was adjusted to exclude noise arising from operation of the hydraulic system.

During the first 1,000 cycles, the acoustic emission was recorded in every 10 or 100 cycles so that the number of counts represented all the events that had taken place in the selected cycles. After the elapse of these cycles, the emission was recorded throughout the remainder of the fatigue process at 1,000-cycle increments. The acoustic emission at a given number of cycles was then the total number of counts measured in a 1,000-cycle period prior to printing.

The signal level of the acoustic emission for the aluminum specimens was very high during the first 10 cycles. This is probably due to changes in specimen gripping due to the downward movement of the lower grip to accommodate the elongation of the specimen under loading. The emission level then decreased gradually and became somewhat stabilized after 1,000 cycles. The emission curves for the specimens subject to stresses 11,400, 11,000, and 10,540 psi are given in figures 10, 11, and 12, respectively. Since the emission in number of counts varies greatly during test, it is impossible to plot the actual numbers on logarithmic scale in the limited space. A simplified

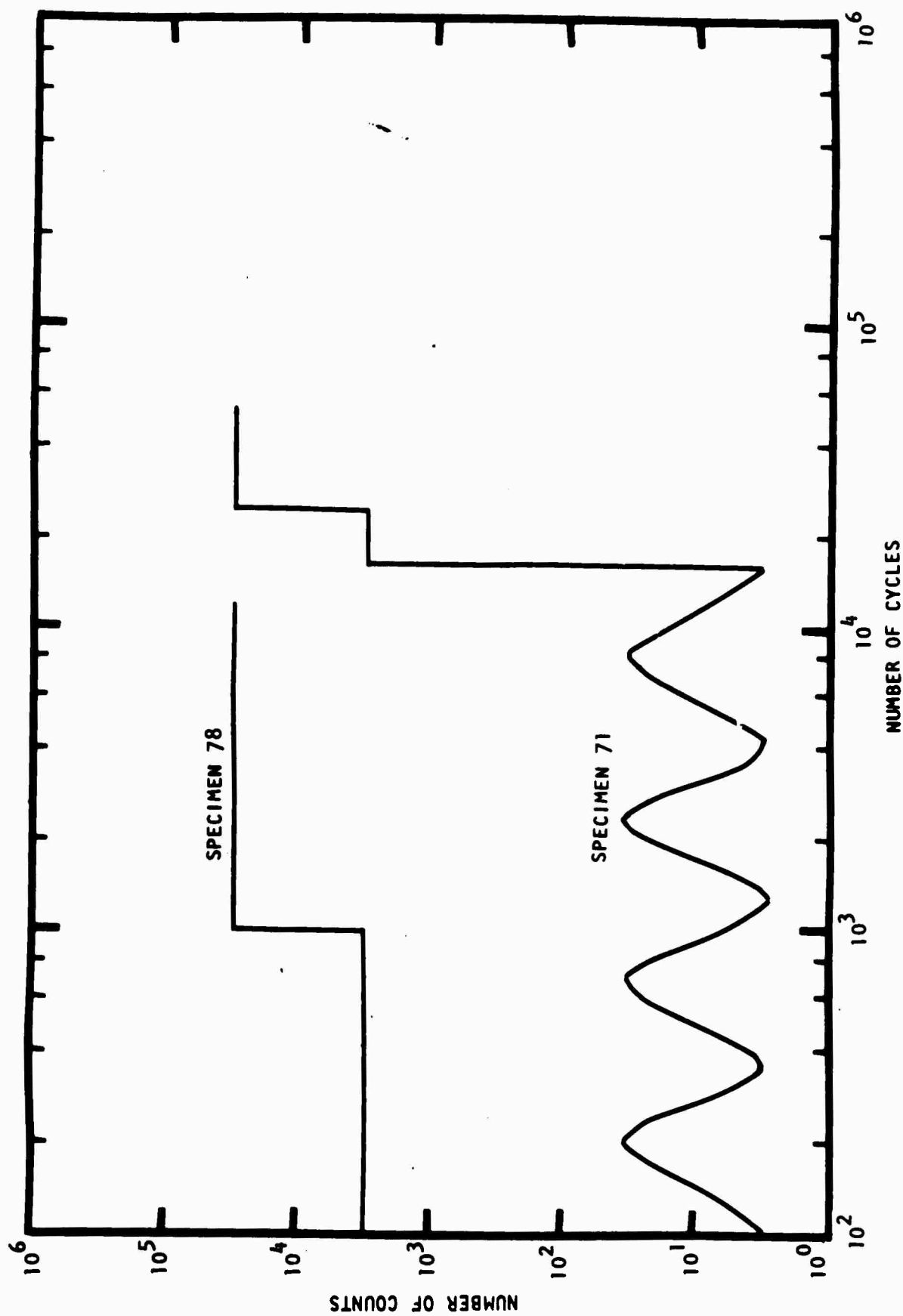


Figure 10. Acoustic Emission of 1100-0 Aluminum in Fatigue Test at 11,400 lb/in.<sup>2</sup>

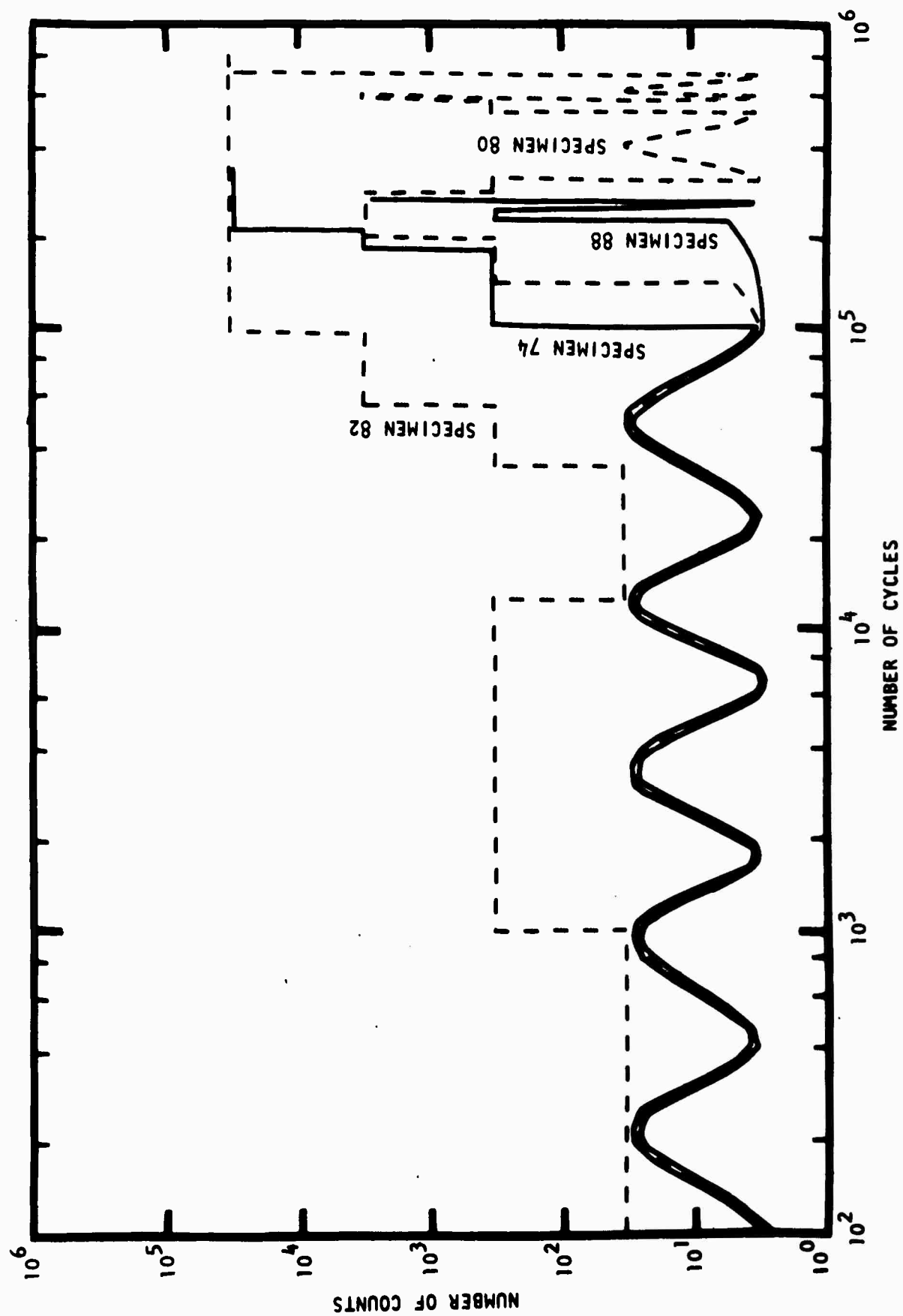


Figure 11. Acoustic Emission of 1100-0 Aluminum in Fatigue Test at 11,000 lb/in.<sup>2</sup>



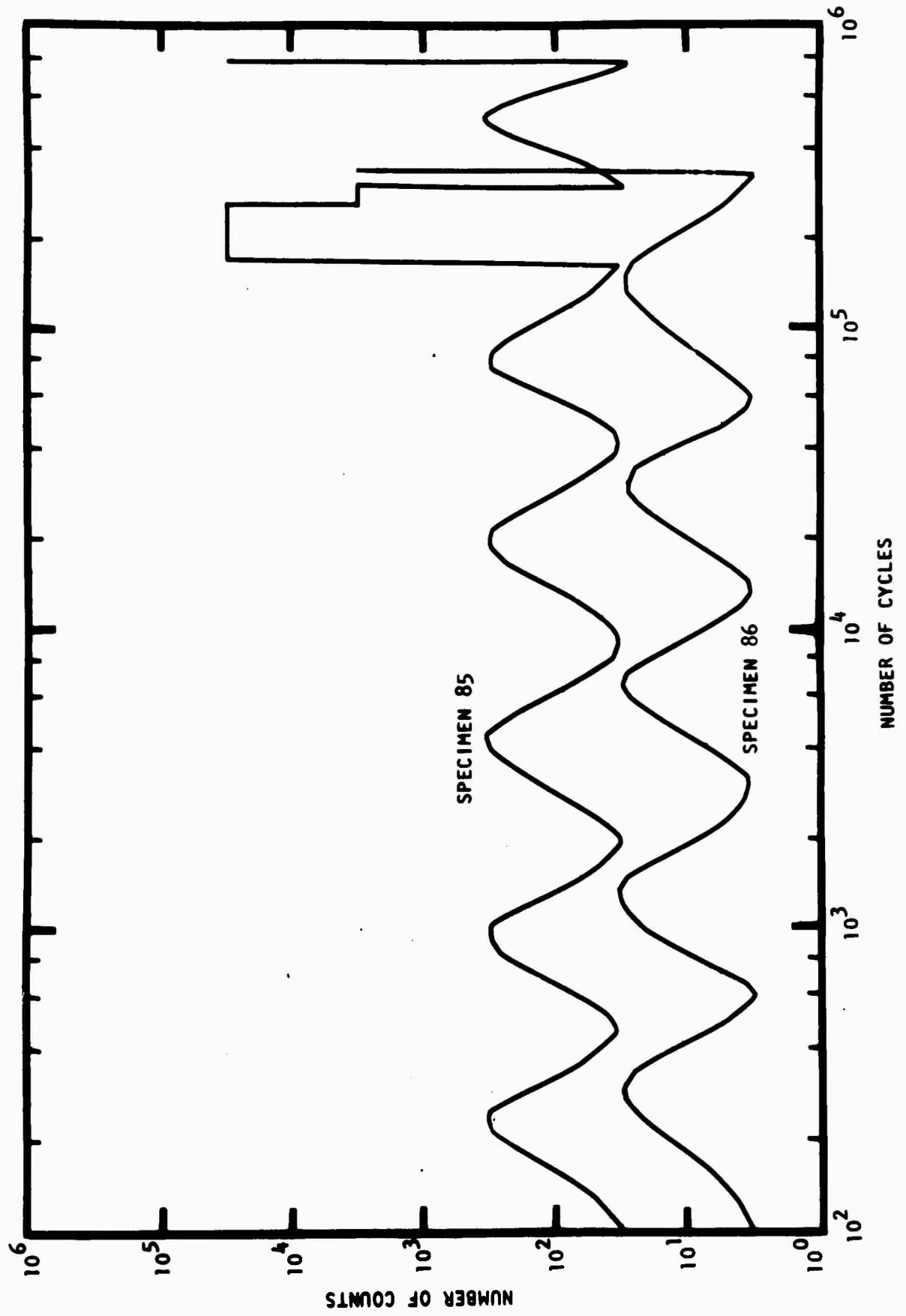


Figure 12. Acoustic Emission of 1100-0 Aluminum in Fatigue Test at 10,540 lb/in.<sup>2</sup>

presentation of the data was made using only the signal variation by the power of 10. The sinusoidal curve centered between the ordinate scales  $10^1$  and  $10^2$  indicates that the number of counts has either one or two digits. A horizontal line signifies that the number of counts is of the same order of magnitude, whereas a vertical line means that the number of counts changes from one order of magnitude to another at the end of the next 1,000 cycles when the recorder prints again.

The acoustic emission intensity, measured in number of counts, can change an order of magnitude several times in the specimen life. Table II summarizes these changes for all the eight 1100-O aluminum specimens. At a high stress level of 11,400 psi, the emission intensity is fairly high throughout the entire life. An increase of one decade in emission from four to five orders of magnitude occurs before half of the life has been spent. At lower stress levels of 11,000 and 10,540 psi, the emission intensity is not only somewhat weaker, but it undergoes several changes in order of magnitude.

In comparing the data presented in table II, it is evident that in seven of the eight tests the acoustic intensity changed by an order of magnitude during the period of 8 to 30 percent of the specimen fatigue life. Further, this is the first significant change noted, and, as such, could be readily flagged as early indicator of fatigue damage. The data scatter for this indicator is about 22 percent, and is most likely accountable to the scatter in actual fatigue failure data. Although this indication is considered most promising, additional tests will be conducted to more firmly establish this

Table II

SUMMARY OF ACOUSTIC EMISSION MEASUREMENT DATA FOR  
1100-O ALUMINUM IN FATIGUE TEST

Specimen	Maximum Stress (psi)	Change of Acoustic Emission by Order of Magnitude	Percentage of Fatigue Life at Start of Emission Change
71	11,400	1 and 2 to 4 4 to 5	30.0 45.0
78	11,400	4 to 5	8.3
74	11,000	1 and 2 to 3 3 to 4 4 to 5	29.0 45.5 60.8
80	11,000	1 and 2 to 3 3 to 4 4 to 3 3 to 1 and 2 1 and 2 to 3 3 to 4 4 to 1 and 2 1 and 2 to 5	20.1 28.7 40.6 46.7 74.6 82.1 84.3 100.0
82	11,000	2 to 3 3 to 2 2 to 3 3 to 4 4 to 5	0.13 1.4 4.4 6.8 11.8
88	11,000	1 and 2 to 3 3 to 1 and 2 1 and 2 to 4	9.2 9.9 100.0
85	10,540	2 and 3 to 5 5 to 4 4 to 2 and 3 2 and 3 to 5	21.9 34.1 39.4 100.0
86	10,540	1 and 2 to 4	100.0

relationship and attempt further correlation between the apparently random variation of the acoustic emission, which occurs after the initial major change and before the emission obviously associated with the crack propagation, and specimen failure.

#### ULTRASONIC METHODS

One of the objectives of this program is to determine the feasibility of detecting early fatigue damage through ultrasonic measurements. It has been established that evidence of fatigue usually appears first at the surface of the material. Very small changes such as microcracks originate within a few microns of the surface and grow until they are large enough to be detected by optical or metallographic methods.

Ultrasonic longitudinal or shear wave signals penetrate the material and generally describe the bulk properties of a material. Surface wave energy, however, travels primarily within one wavelength of the surface. To increase the relative importance of phenomena at the surface, the depth of penetration should be as small as possible. High frequency produces short wavelength and gives added importance to variations at the surface.

The initial investigation using surface wave measurements was performed at frequencies of 10 MHz and lower because higher frequency transducers were not available. The wavelength at 10 MHz is about 0.012 inch or 300 microns for surface waves in aluminum. Sources were sought for surface wave transducers to operate at 60 MHz where the wavelength and, therefore, the penetration would be approximately 0.002 inch or 50 microns. Several manufacturers

have made experimental units to operate as high as 30 MHz. Two companies, Panametrics and Nortec, have offered to design and build higher frequency units as special items. The Science Center of North American Rockwell Corporation has had experience with surface wave measurements using both commercial units where available and developing new techniques for special tests. Other sources are being investigated and several transducers used by Tracor, Inc, for similar measurements were evaluated. Some of these units are presently inoperative, and none have been found to operate as well as available commercial transducers.

An unmounted shear wave crystal made of Y-cut quartz has been obtained with a nominal natural frequency of 50 MHz. This crystal will be mounted on a plastic wedge to make an experimental surface wave transducer using mode conversion.

Both velocity and attenuation of the surface wave are being considered as possible indicators of fatigue. The microcracks and slip lines are very small and probably do not have high density in early stages of fatigue. A change in the ultrasonic velocity or attenuation may be affected by microcracking, stress, etc, during the fatigue process.

The two primary problems currently being studied are (1) how to propagate well-defined high-frequency ultrasonic signals into and out of the specimens, and (2) how to measure the velocity or attenuation with sufficient accuracy to give definitive measurements of small changes.

Time measurements required for velocity have traditionally been made using a sharp pulse or step function as the ultrasonic signal. This type of signal consists not of one frequency, but of a broad band of frequencies. Since wavelength is different for each frequency component, the depth of penetration is not easily defined. An alternate method of time measurement is to use continuous-wave signals at a known frequency and measure phase difference in a known travel distance.

The selection of transducers includes consideration of test frequency, signal damping and acoustic coupling method. Mode conversion wedges tend to ring or reflect badly, and the coupling changes substantially with either small differences in applied pressure or small changes in material. The signal pattern can be changed very significantly by shifting the pressure from the front to the back of the transducer or by varying the amount of couplant. The optimum wedge angle also changes with the velocity in the specimen. The importance of this effect increases directly with frequency.

Several other coupling methods are being considered. A comb or ridged surface coupling with points of contact spaced an integral number of wavelengths can be used in some applications. It becomes very difficult to space these ridges only 0.002 inch as they would need to be at 60 MHz. Microwave ultrasonic delay lines are being made by etching interdigital electrode patterns on  $\text{LiNO}_3$  crystals. This performs essentially the same job as the comb and provides good surface waves in the crystal, but there seems to be no good way to couple the energy into a metal test specimen. An alternate method

converts longitudinal waves to surface waves in an immersion tank. With the specimen immersed in liquid, the attenuation is high.

After surface waves have been generated in the test specimen, there are several methods by which acoustic signal characteristics can be measured to determine velocity and attenuation.

Wedge or comb transducers can be used for transmitters or receivers. Another type of transducer system suitable for receiving only is available using the Tracor laser system. A narrow beam of light from a HeNe laser is focused on the specimen. As a surface wave passes this point, the light beam is disturbed. Detection may be accomplished by several means. An interference or heterodyne pattern between direct and reflected light can be detected by the photodetector. Motion much less than one wavelength of light can be measured. Another detection method takes advantage of the fact that surface waves change the angle of the surface. The reflected light can be passed through a diffraction grating or split by a knife edge to cause relatively large variations in light intensity at the photodetector for small angular deflections.

When the time delay and signal amplitude have been measured at one location on the specimen, the length of the signal path can be changed by a known increment and a second reading taken. Velocity and attenuation readings can be based on changes in travel time and signal amplitude. Signal amplitude is strongly influenced by coupling efficiencies and repeatability of setup procedures. Methods are being sought to improve the repeatability and accuracy of attenuation measurements.

Time measurements can be made very accurately, but this advantage is partly offset by the fact that velocities are not expected to change much. If velocity differences between fatigued and unfatigued specimens are very small, it will be necessary to measure both distance and time very accurately. A method is being considered which would use phase measurements for both distance and time. If both the laser light frequency and the excitation ultrasonic frequency are known very precisely they can be used to accurately determine the other variables.

The accurate measurement of distance by means of laser light and interference patterns is well established. The distance a specimen is moved can be determined by the number of wavelengths gained or lost in a heterodyne system. Using a similar technique, the phase shift of the ultrasonic signal can be measured over the known distance. The number of full cycles plus the angular proportion of a partial cycle can be determined. Knowing the distance moved and the exact phase shift of the ultrasonic signal, we can establish the wavelength of the surface wave. Knowing wavelength and ultrasonic frequency, the velocity is easily determined.

#### METALLOGRAPHIC EXAMINATION

Metallographic examination using an optical microscope and an electron microscope was conducted on the six electropolished 1100-O aluminum specimens. One was a control while the other five had been subject to fatigue deformation at a maximum stress 11,000 psi for  $5 \times 10^3$ ,  $1 \times 10^4$ ,  $5 \times 10^4$ ,



$1 \times 10^5$ , and  $2 \times 10^5$  cycles. Since the average fatigue life at this stress level is  $3 \times 10^5$  cycles, the percentages of the spent life for the five specimens are 1.3, 3.3, 16.7, 33.3, and 66.7.

The optical micrographs and electron micrographs for the six specimens are reproduced in figures 13 and 14, respectively. The control surface shows a relatively smooth grain structure. The fatigued specimen surface exhibits considerable evidence of slip. Slip lines or bands are visible on the surface of the specimen which had spent only about 1.3 percent of the life. These slip lines are a little widely separated from one another. As the number of cycles increases, the width between slip lines becomes narrower.

The early appearance of slip lines or bands on the fatigue-deformed surface does not necessarily indicate fatigue damage, since only those slip bands that are resistant to removal are thought to be the potential nucleation sites for fatigue cracks. The presence of the persistent bands are usually ascertained by successive removal of deformed surface layers. The removal is better performed under secondary electron emission microscope, using gas etching, because the rate of removal is constant and the fresh, new surface can be examined in the etching process. This work is now in progress.

#### FATIGUE TESTS

The average fatigue life of 7075-T6 aluminum alloys at two maximum stress levels (40,000 and 6,000 psi) was determined to be  $3.3 \times 10^4$  and  $2.5 \times 10^6$  cycles, respectively. Three specimens each were then fatigue tested at these

NOT REPRODUCIBLE



CONTROL, 0 CYCLE

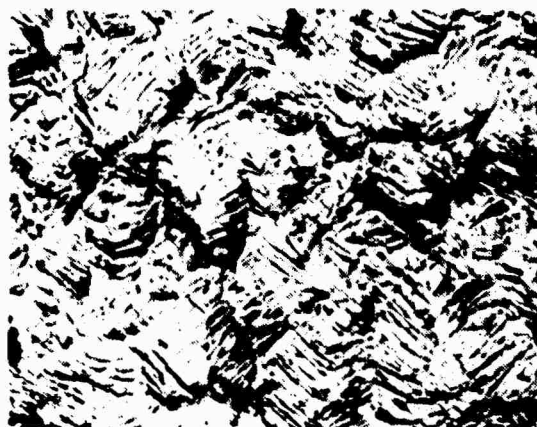
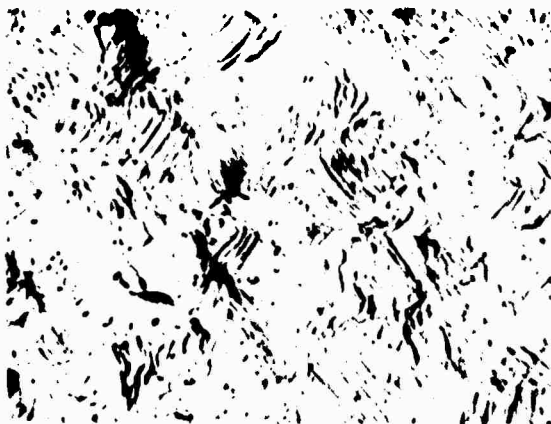
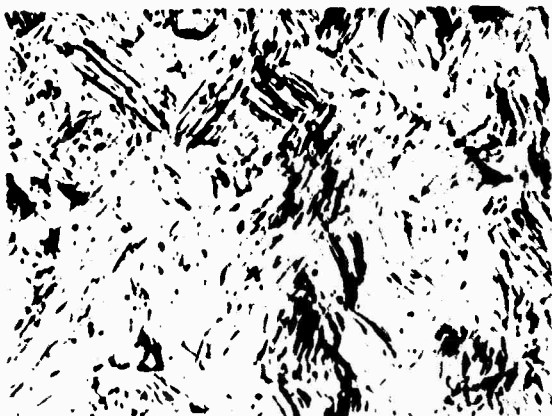
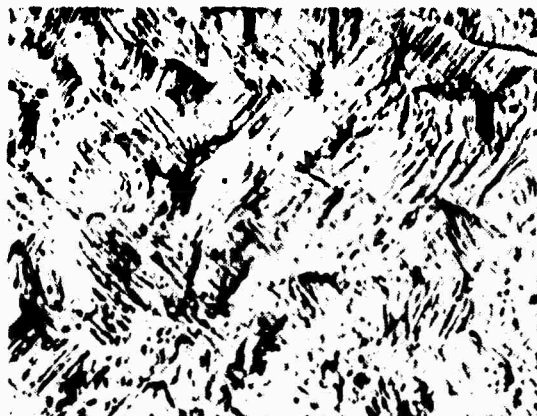
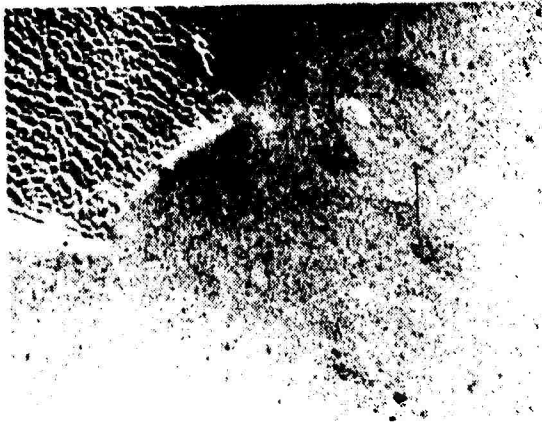
 $5 \times 10^4$  CYCLES $5 \times 10^3$  CYCLES $1 \times 10^5$  CYCLES $1 \times 10^4$  CYCLES $2 \times 10^5$  CYCLES

Figure 13. Optical Micrographs of Fatigued 1100-0 Aluminum Specimens (250X)



CONTROL, 0 CYCLE

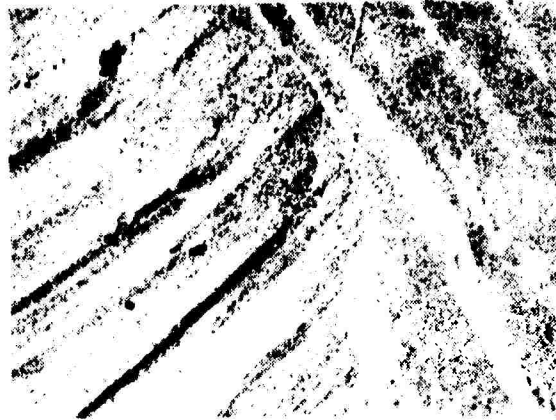
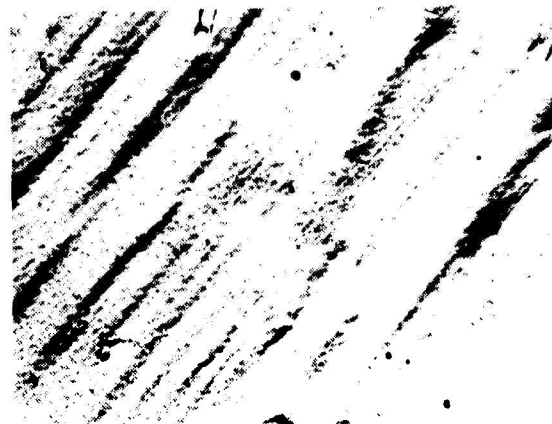
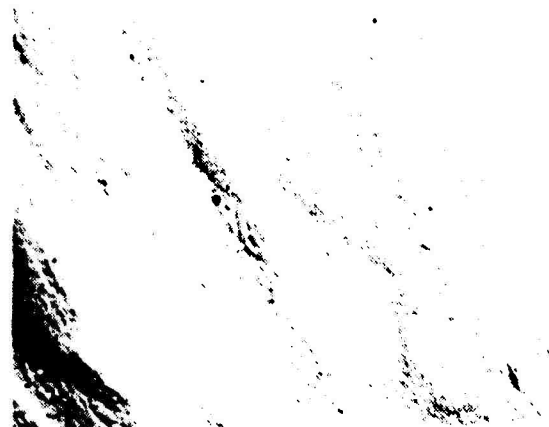
 $5 \times 10^4$  CYCLES $5 \times 10^3$  CYCLES $1 \times 10^5$  CYCLES $1 \times 10^4$  CYCLES $2 \times 10^5$  CYCLES

Figure 14. Electron Micrographs of Fatigued 1100-0 Aluminum Specimens (6,400X)

stress levels for 2, 5, 10, and 25 percent of the life. The fatigued specimens will be used in ultrasonic tests to correlate fatigue damage with material response to the propagation of surface waves.

## Section V

## SUMMARY AND CONCLUSIONS

The exoelectron emission current was characterized in air in terms of the fatigue deformation of 1100-O aluminum. The current level increases soon after the start of the test, reaching a peak in the first hundred cycles. Thereafter, it decreases steadily for the most part of the remaining fatigue life. Near the end of the life, a slow and then rapid rise of current is observed. This rise is attributed to the formation and propagation of fatigue cracks, leading to complete specimen failure. The variation of the change of emission current, relative to the current after the elapse of a few hundred or a few thousand cycles, with time tends to be independent of applied stress levels. This relationship offers a means to assess the accrued damage as well as to predict the remaining safe life of the fatigued material.

The acoustic emission of 1100-O aluminum was measured concurrently with exoelectron emission tests. The intensity of the acoustic emission, expressed in number of counts in 1,000 cycles, appears to vary by several orders of magnitudes during the test. An apparent relationship was established between the first significant emission level change and the percent of fatigue life. The change occurs during the early portion of the fatigue life (8 to 30 percent) and offers a possible early fatigue damage warning. Other acoustic emission tests and characterizations are needed to verify this relationship and clarify the meaning of subsequent emissions prior to the failure-related emission activity.

Metallographic examination of fatigued 1100-O aluminum specimens reveals that slip bands appear at as early as 1.3 percent of the fatigue life, when the maximum applied stress is 11,000 psi. The bands become more dense with increasing number of cycles.

## Section VI

## FUTURE WORK

During the next report period, the following major tasks are planned:

1. Investigation of the effect of heat on exoelectron emission. The emission current of the five 1100-O aluminum specimens which had been fatigue stressed to various percentages of the life will be measured while they are being heated up to 194° F (90° C).
2. Continued investigation of the exoelectron emission in air using 7075-T6 aluminum alloy, D6AC steel, and 6Al-4V titanium alloy specimens. The change of current-percentage of fatigue life relationship observed in tests on 100-O aluminum will be checked.
3. Concurrent measurement of acoustic emission with exoelectron emission to establish and confirm the relationship between acoustic emission and spent fatigue life.
4. Evaluation of the response of fatigued 7075-T6 aluminum alloy and D6AC steel to the propagation of ultrasonic surface waves.